



## Electrochemical xanthine biosensor based on zinc oxide nanoparticles–multiwalled carbon nanotubes–1,4-benzoquinone composite

Berna Dalkıran<sup>1</sup>, Ceren Kaçar<sup>1</sup>, Pınar Esra Erden<sup>1,2</sup>, Esmâ Kılıç<sup>1</sup>

<sup>1</sup>Ankara University, Faculty of Science, Department of Chemistry, Ankara, TURKEY

<sup>2</sup>Gazi University, Polatlı Faculty of Science and Arts, Department of Chemistry, Ankara, TURKEY

**Abstract:** Zinc oxide nanoparticles (ZnONPs), multiwalled carbon nanotubes (MWCNTs) and 1,4-benzoquinone (BQ) dispersed in chitosan (CS) matrix were used to construct a xanthine biosensor. Xanthine oxidase (XOx) was immobilized onto BQ-MWCNTs-ZnO-CS composite modified glassy carbon electrode (GCE) using glutaraldehyde as the crosslinking agent. The parameters of the construction process and the experimental variables for the biosensor were optimized. The xanthine biosensor showed optimum response within 10 s, and the sensitivity was 39.4  $\mu\text{A}/\text{mMcm}^2$  at +0.25 V (vs. Ag/AgCl). The linear working range of the biosensor was found to be  $9.0 \times 10^{-7}$ – $1.1 \times 10^{-4}$  M with a detection limit of  $2.1 \times 10^{-7}$  M. The biosensor exhibited good long-term stability and reproducibility. The presented biosensor was also used for monitoring the freshnesses of chicken and beef flesh.

**Keywords:** Xanthine, biosensor, zinc oxide nanoparticles, carbon nanotubes, mediator.

**Submitted:** April 21, 2017. **Accepted:** January 19, 2018.

**Cite this:** Dalkıran B, Kaçar C, Erden P, Kılıç E. Electrochemical xanthine biosensor based on zinc oxide nanoparticles–multiwalled carbon nanotubes–1,4-benzoquinone composite. JOTCSA. 2018;5(1):317–32.

**DOI:** To be assigned.

**\*Corresponding author. E-mail:** bernadalkiran@gmail.com.

## INTRODUCTION

Xanthine concentration in biological fluids is used as an index for the diagnosis of various disorders such as xanthinuria, renal failure and gout. Moreover, xanthine attracted much attention as a marker for estimating the meat freshness in food industry (1). Therefore, direct, rapid, accurate and low cost measurement of xanthine in samples is of great interest in clinical analysis and food industry. Electrochemical enzyme electrodes that combine the sensitivity of electroanalytical methods with the bioselectivity of the enzyme are promising alternatives for sensitive, specific and rapid determination of xanthine (2).

Carbon nanotubes (CNTs) have been widely used in biosensor applications due to their unique properties such as high electrocatalytic effect, large surface area, mechanical strength, chemical stability, strong adsorption ability and biocompatibility (3, 4). Nowadays, the modification of CNTs with other nanomaterials such as metal or metal oxide nanoparticles (MONPs) is of great importance since the composite materials possess characteristics of the individual constituents and have favorable synergistic effects (5, 6). It is well known that ZnO is a semiconductor with band gap of 3.37 eV and has some beneficial electronic and optical properties. ZnO nanoparticles also have potential in biosensing applications because of their unusual features including rapid electron transfer ability, chemical stability, biocompatibility, large surface area, high catalytic efficiency, non-toxicity, and strong adsorption ability (7, 8). ZnONPs and MWCNTs composite has already used in fabricating biosensors. Wang *et al.*, reported the development of a lactate biosensor based on the synergistic action of MWCNTs and ZnONPs (9). Palanisamy *et al.*, immobilized hemoglobin at MWCNTs/ZnO composite modified GCE to develop an amperometric biosensor for H<sub>2</sub>O<sub>2</sub> determination (7). Haghghi and Bozorgzadeh decorated ZnONPs on MWCNTs to construct an electrochemiluminescence lactate biosensor (10). Ma and Tian fabricated a hemoglobin biosensor based on ZnO coated MWCNTs and nafion composite and studied the direct electron transfer and electrocatalysis of hemoglobin (11). Zhang *et al.*, reported a ZnO/MWCNTs/CS nanocomposite based electrochemical DNA biosensor (12). Hu *et al.*, constructed a glucose biosensor based on ZnO nanoparticle and MWCNTs modified GCE and investigated the direct electron transfer of glucose oxidase enzyme (13).

The catalytic oxidation of xanthine in the presence of XOx enzyme takes place according to the following equation:



Electrooxidation of H<sub>2</sub>O<sub>2</sub> generated by the enzymatic reaction is widely used for the amperometric determination of xanthine (14). High potentials used for the electrooxidation of H<sub>2</sub>O<sub>2</sub> make the electrode sensitive to common interferences. The use of artificial electron transfer mediators including Prussian blue, colloidal gold, ferrocene and its derivatives, cobalt phthalocyanine and ferricyanide to

eliminate the influence of interferences is a common approach in xanthine enzyme electrodes (15, 16, 17, 18).

Herein, we report a novel biosensor based on MWCNTs, ZnONPs and BQ composite. Such composite is expected to give enhanced response characteristics towards xanthine due to the synergic action of its components. Moreover, the use of BQ is expected to provide an interference free biosensor by lowering the operating potential. To the best of our knowledge, no study has yet been published based on the MWCNTs, ZnONPs and BQ composite for the amperometric detection of xanthine.

## MATERIALS AND METHODS

### Reagents

XOx from Microbial source, ZnONPs (<100 nm particle size (TEM)),  $K_3Fe(CN)_6$ ,  $K_4Fe(CN)_6 \cdot 3H_2O$ , uric acid, sodium dihydrogen phosphate dihydrate, glutaraldehyde, disodium hydrogen phosphate dihydrate, Nafion, sodium benzoate, creatine, caffeine, theophylline and ascorbic acid were obtained from Sigma (St. Louis, MO, USA). Xanthine, BQ and glucose were purchased from Fluka (Buchs, Switzerland). MWCNTs (O.D. <8 nm; I.D. 2–5 nm; length 10–30  $\mu m$ ) were bought from Cheaptubes Inc. (Brattleboro, USA). CS (medium molecular weight) was obtained from Aldrich. Standard xanthine solution was prepared by dissolving xanthine in 0.10 M NaOH. All aqueous solutions were prepared using deionized water.

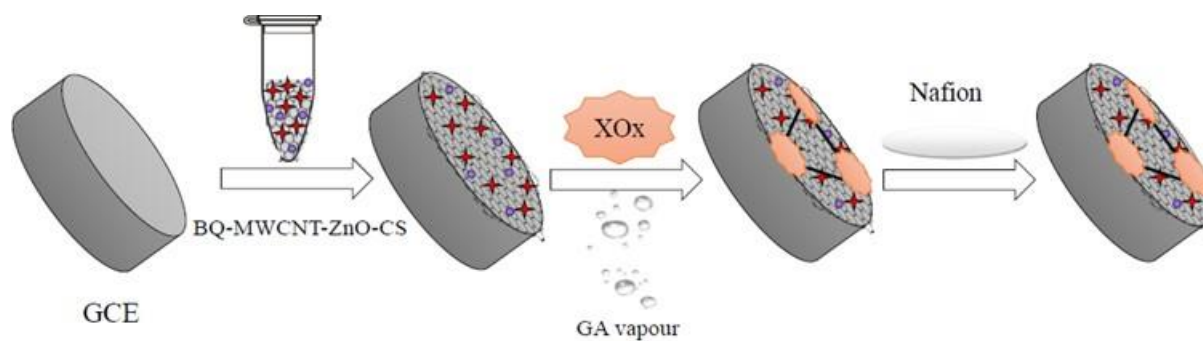
### Apparatus

Electrochemical studies were carried out in a three-electrode cell. Ag/AgCl electrode, platinum wire and GCE were employed as reference, counter and working electrodes, respectively. The electrochemical setup also involved a computerized IviumStat.h electrochemical analyzer (Ivium Technologies, Netherlands). Scanning electron microscopy (SEM) images were taken from Carl Zeiss AG, EVO® 50 Series. 0.1 M KCl aqueous solution containing 5.0 mM  $K_3[(Fe(CN)_6)]$ , 5.0 mM  $K_4[(Fe(CN)_6)]$  (redox probe) was used for the cyclic voltammetry (CV) and electrochemical impedance spectroscopy (EIS) experiments. Cyclic voltammograms (CVs) were recorded between (-1.0)–(+1.0)V at a scan rate of 50  $mV s^{-1}$ . EIS experiments were conducted with a frequency range of  $10^6$ –0.5 Hz under open circuit potential ( $E_{OCP}$ ) conditions (0.2 V). Phosphate buffer solution (PBS; 0.05 M pH 7.5) was the supporting electrolyte for the amperometric measurements.

### Enzyme Electrode Preparation

In this study, modified and unmodified GCEs were used as working electrodes. GCE was polished according to the procedure reported elsewhere (19). 0.50 g CS was dissolved in 50.0 mL acetate buffer solution (pH 5.0) under magnetic stirring. 10 mg MWCNTs and 10 mg ZnONPs were ultrasonicated in 10.0 mL CS solution to achieve a final concentration of 1  $mg mL^{-1}$  MWCNTs and 1  $mg mL^{-1}$  ZnONPs. 10 mg BQ was added to MWCNTs-ZnO-CS mixture and ultrasonicated. 10  $\mu L$  of the

BQ-MWCNTs-ZnO-CS mixture was cast onto the GCE surface and allowed to dry for 2 h at room temperature. 10  $\mu\text{L}$  XOx solution ( $0.025 \text{ Units } \mu\text{L}^{-1}$ ) was drop-cast on BQ-MWCNTs-ZnO-CS/GCE surface and allowed to dry. XOx/BQ-MWCNTs-ZnO-CS/GCE was treated with glutaraldehyde vapor for 10 min to achieve the crosslinking of the enzymes. 7.5  $\mu\text{L}$  Nafion solution (0.25%) was cast on the resulting electrode and dried. The fabrication procedure of the xanthine biosensor is shown in Scheme 1.



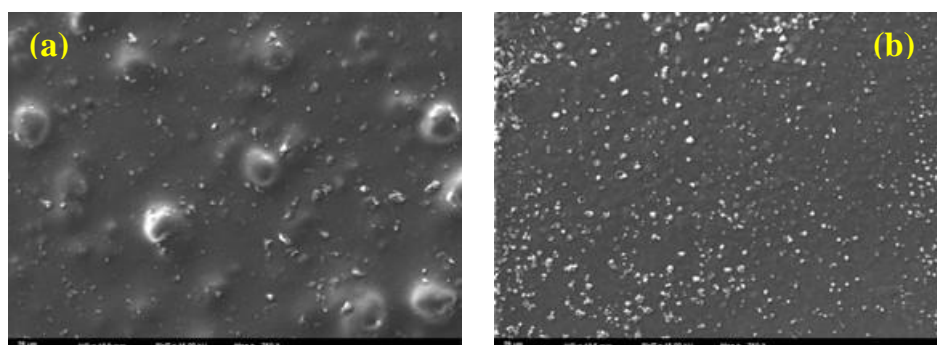
**Scheme 1.** The fabrication procedure for the XOx/BQ-MWCNTs-ZnO-CS/GCE.



## RESULTS AND DISCUSSION

### Morphological studies

SEM images of (a) ZnO-CS/GCE, (b) BQ-CS/GCE, (c) MWCNTs-ZnO-CS/GCE, (d) BQ-MWCNTs-ZnO-CS/GCE and (e) XOx/BQ-MWCNTs-ZnO-CS/GCE are depicted in Figure 1. Images a and b show that ZnONPs or BQ are well dispersed in CS matrix. In image c structures corresponding to MWCNTs and ZnONPs can be seen. The porous structure of the resulting BQ-MWCNTs-ZnO composite (image d) is very suitable for enzyme immobilization. After XOx immobilization the porous structure of the BQ-MWCNTs-ZnO-CS composite changed to a more regular form (image e).



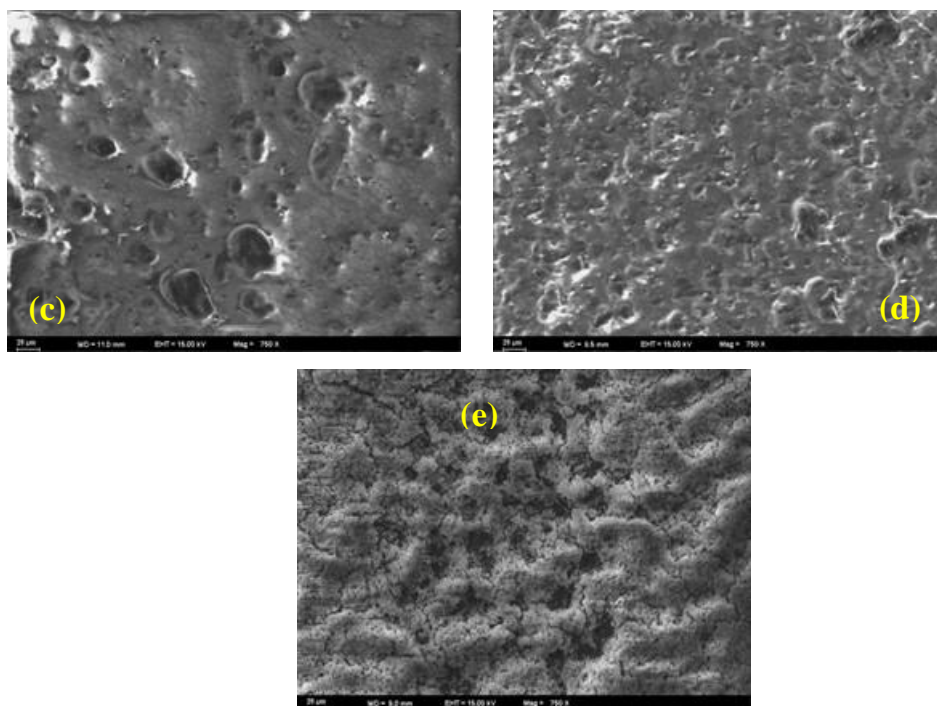


**Figure 1.** SEM images of (a) ZnO-CS/GCE, (b) BQ-CS/GCE, (c) ZnO-MWCNTs-CS/GCE, (d) BQ-MWCNTs-ZnO-CS/GCE, (e) XOx/BQ-MWCNTs-ZnO-CS/GCE (20  $\mu\text{m}$ ; EHT = 15.00 kV; Mag = 750 $\times$ )

### Electrochemical studies

Electrochemical characteristics of the modified and unmodified electrodes were investigated by CV and EIS studies. Figure 2A shows the CVs recorded for BQ-MWCNTs-ZnO-CS/GCE (curve a) and XOx/BQ-MWCNTs-ZnO-CS/GCE (curve b) in  $[\text{Fe}(\text{CN})_6]^{3-/4-}$  redox probe. Oxidation and reduction peaks corresponding to the redox probe were obtained at BQ-MWCNTs-ZnO-CS composite modified GCE (curve a). After the XOx enzyme was introduced into the composite peak currents decreased dramatically indicating that the immobilized enzyme layer hindered the electron transfer (curve b) (20).

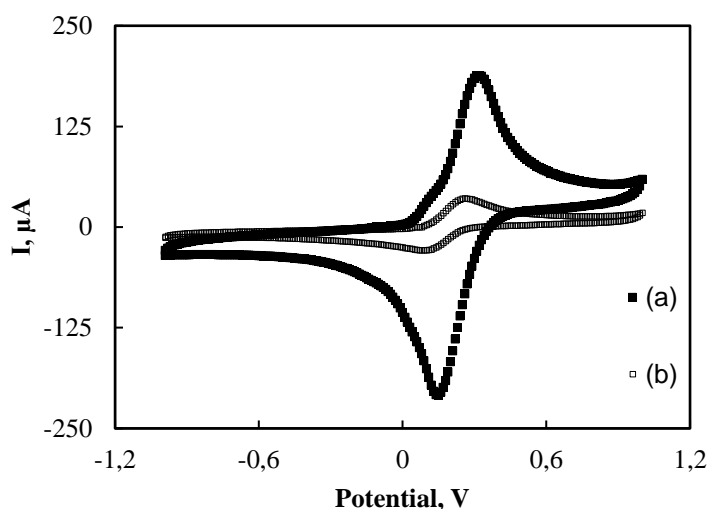


**Figure 2A.** CVs of (a) BQ-MWCNTs-ZnO-CS/GCE and (b) XOx/BQ-MWCNTs-ZnO-CS/GCE in 0.10 M KCl solution containing 5.0 mM  $\text{Fe}(\text{CN})_6^{3-/4-}$  at 50  $\text{mVs}^{-1}$ .

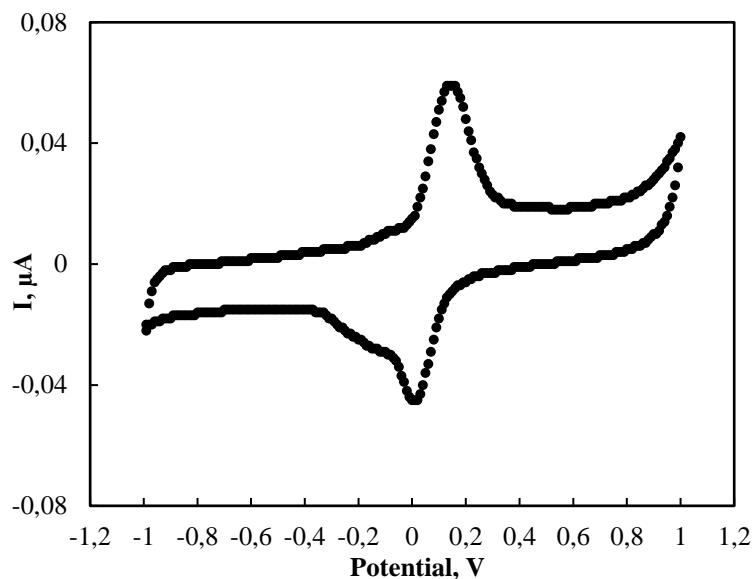


**Figure 2B.** CV of BQ-MWCNTs-ZnO-CS/GCE in 0.05 M PBS containing 0.1 M KCl at 50 mVs<sup>-1</sup>.

The CV of BQ-MWCNTs-ZnO-CS/GCE recorded in 0.05 M PBS containing 0.1 M KCl (Figure 2B) exhibited one anodic peak ( $E_{pa} = +0.18$  V) at forward scan of the potential and one cathodic peak ( $E_{pc} = +0.02$  V) at backward scan of the potential. These peaks correspond to the oxidation and reduction peaks of BQ (21).

The Nyquist plot (Figure 3) shows EIS studies of unmodified GCE (curve a), BQ-MWCNTs-ZnO-CS/GCE (curve b) and XOx/BQ-MWCNTs-ZnO-CS/GCE (curve c). In Nyquist plot the diameter of the semicircle portion at higher frequencies corresponds to the charge transfer resistance ( $R_{ct}$ ), which controls the electron transfer kinetics of the redox probe at the electrode interface (22). In our study the  $R_{ct}$  of BQ-MWCNTs-ZnO-CS/GCE (55  $\Omega$ ) was found to be lower than the  $R_{ct}$  of the bare GCE (1250  $\Omega$ ). This indicates a decreased resistance and improved electron transfer efficiency for the BQ-MWCNTs-ZnO-CS/GCE. After immobilization of XOx onto BQ-MWCNTs-ZnO-CS composite, the value of  $R_{ct}$  increased to 480  $\Omega$  revealing that the immobilization of XOx cause hindrance to electron transfer due to the insulating property of the enzyme. The increase in  $R_{ct}$  further confirms the successful immobilization of the enzymes onto the BQ-MWCNTs-ZnO-CS composite.

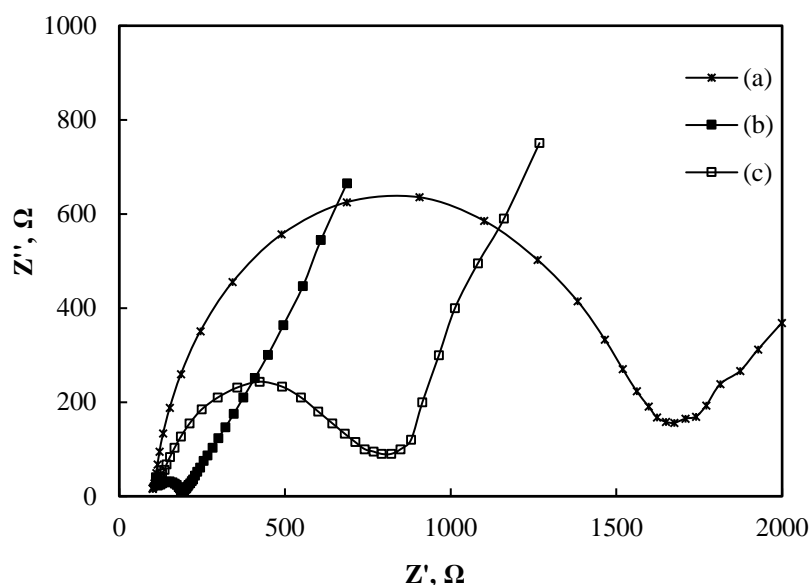


**Figure 3.** The Nyquist curves of in (a) unmodified GCE, (b) BQ-MWCNTs-ZnO-CS/GCE and (c) XO<sub>x</sub>/BQ-MWCNTs-ZnO-CS/GCE in 0.10 M KCl solution containing 5.0 mM Fe(CN)<sub>6</sub><sup>3-/4-</sup>.

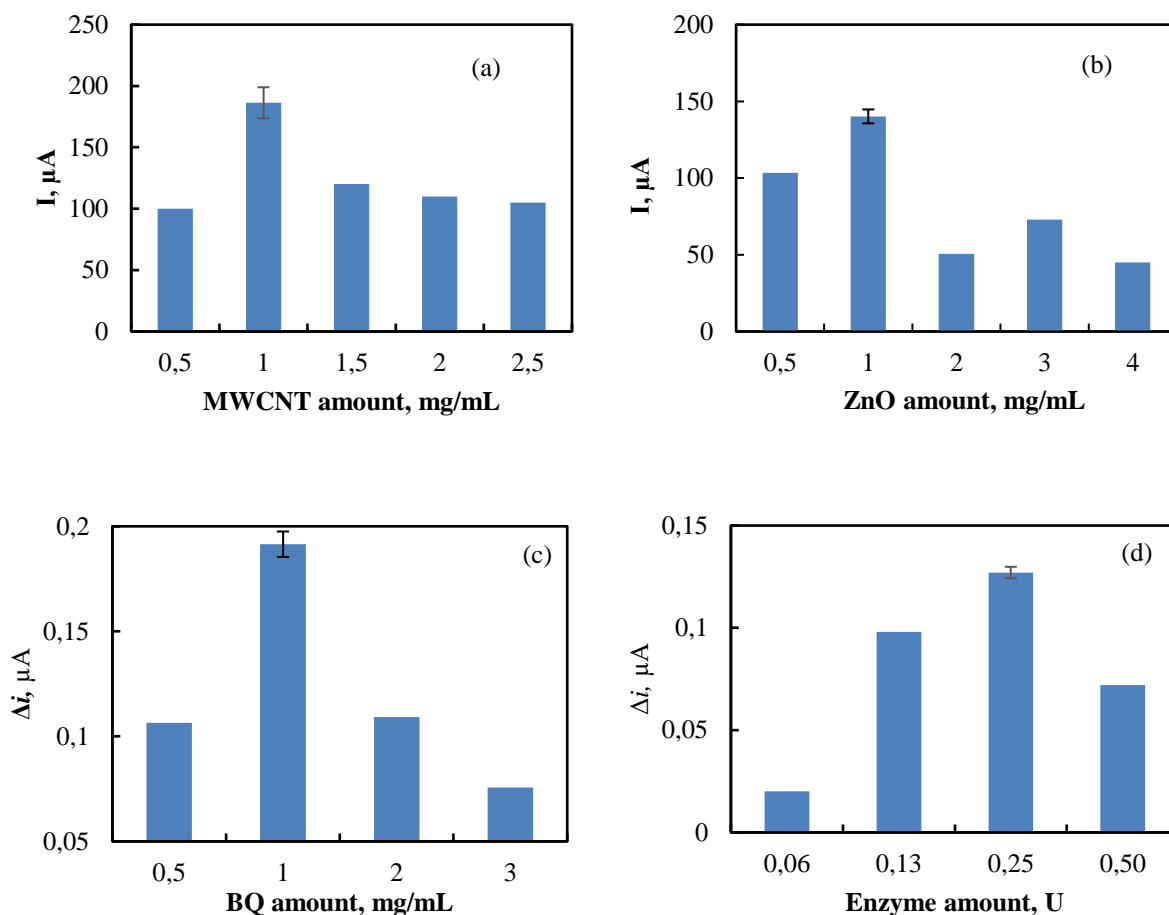
### Optimization studies

Effects of MWCNTs, ZnONPs, BQ and enzyme amount were studied in order to optimize the composition of the biosensor. All optimization studies were conducted in 0.05 M PBS (pH 7.5) containing 0.05 mM xanthine and response currents of the biosensor were recorded. Effect of MWCNTs amount on biosensor response was investigated using different MWCNTs amounts as 0.5 mg mL<sup>-1</sup>; 1.0 mg mL<sup>-1</sup>; 1.5 mg mL<sup>-1</sup>; 2.0 mg mL<sup>-1</sup> and 2.5 mg mL<sup>-1</sup>. 10 μL of these solutions were used for electrode construction and the amperometric response of the electrodes were recorded. The highest current response was observed with the electrode prepared with 1.0 mg mL<sup>-1</sup> MWCNTs and this value was selected as the optimum MWCNTs amount. MWCNTs amounts higher than 1.0 mg mL<sup>-1</sup> did not increase the biosensor response.

Different ZnONPs amounts from 0.5 mg mL<sup>-1</sup> to 4.0 mg mL<sup>-1</sup> were used for biosensor construction to study the the effect of ZnONPs amount on biosensor response. The highest biosensor response was obtained with 1.0 mg mL<sup>-1</sup> ZnONPs and this value was used for all further experiments. BQ amount was varied between 0.5 mg mL<sup>-1</sup> and 3 mg mL<sup>-1</sup> to optimize the mediator amount. The response current of the biosensor increased with the mediator amount up to 1 mg mL<sup>-1</sup> and then decreased with increasing BQ amount. Therefore, 1.0 mg mL<sup>-1</sup> BQ was used for biosensor construction. The decrease in the response current of the biosensor at high MWCNTs, ZnONPs or BQ concentrations could be due to an increase in the diffusion barrier for the electroactive species toward electrode surface (6-19).

Various XO<sub>x</sub> amounts (0.06; 0.12; 0.25 and 0.50 U) were immobilized onto the BQ-MWCNTs-ZnO-CS/GCE to optimize the enzyme amount (Figure 4). It is clear from the figure that the response current increased from 0.06 to 0.25 U and then decreased. The highest response current was recorded with

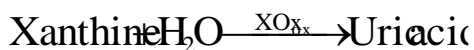
0.25 U XOx and this value was selected as the optimum enzyme loading. The current decrease at higher enzyme loading (>0.25 U) may be attributed to the blocking of the electrode surface by the large amount of immobilized protein (23, 24).

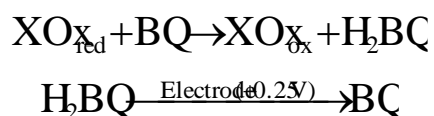


**Figure 4.** Effects of (a) MWCNTs, (b) ZnONPs, (c) BQ and (d) XOx amount on the response of the XOx/BQ-MWCNTs-ZnO-CS/GCE (in 0.05 M PBS at +0.25 V, error bars indicate the standard deviation of three measurements).

Operating potential is another critical parameter for biosensor response and selectivity. The amperometric response of the xanthine biosensor to 0.05 mM xanthine was measured at different operating potentials between (+0.10)–(+0.30) V. This potential range was selected due to the oxidation and reduction peaks of BQ (Figure 2B). The highest biosensor response was recorded at +0.25 V (data not shown). Therefore, all further measurements were performed at +0.25 V.

In this study, we have used BQ as the artificial electron transfer mediator in order to minimize the effects of common interfering substances normally present in real samples. The purposed response mechanism for the XOx/BQ-MWCNTs-ZnO-CS/GCE can be illustrated as follows:





In the response mechanism of the presented biosensor BQ accepts electrons from the reduced XOx and H<sub>2</sub>BQ is produced. At an operating potential of +0.25 V H<sub>2</sub>BQ is reoxidized to form BQ on the surface of the electrode. The current is directly proportional to xanthine concentration.

The effect of pH on biosensor response was studied in the pH range of 6.0-8.5 in the presence of 0.05 mM xanthine. Figure 5 shows that the optimum response current was obtained at pH 7.5, and this pH was selected as the optimum pH. This value is compatible with the pH values reported for the previous xanthine biosensors (25-27).

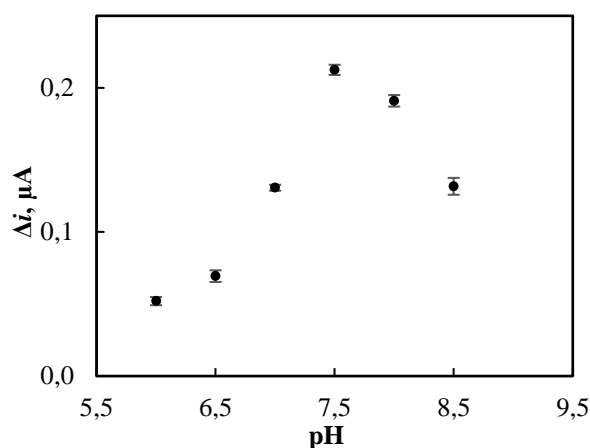


**Figure 5.** Effect of pH on the response of the XOx/BQ-MWCNTs-ZnO-CS/GCE (in 0.05 M PBS at +0.25 V, error bars indicate the standard deviation of three measurements)

### Analytical characteristics

The amperometric response of the biosensor to successive injection of xanthine was studied. The biosensor showed a fast response to xanthine and achieved 95% of steady current within 10 s. The relationship between response current (μA) and xanthine concentration was linear from  $9.0 \times 10^{-7}$  to  $1.1 \times 10^{-4}$  M with the linear equation being  $\Delta i = 2.80 c + 0.02$  ( $R^2=0.992$ ) (Figure 6). Detection limit of the xanthine biosensor was calculated according to the  $3S_b/m$  criterion where  $m$  is the slope of the calibration curve and  $S_b$  was estimated as the standard deviation of 10 different amperometric signals recorded for the lowest xanthine concentration (0.9 μM) in the linear range and found as  $2.1 \times 10^{-7}$  M (28). The sensitivity of the biosensor was found to be  $39.4 \mu\text{A}/\text{mMcm}^2$ . This detection limit is much lower than the detection limits obtained in previously reported xanthine biosensors (17, 29, 30). Similar detection limits for xanthine biosensors were also reported in the literature (1, 31, 32).

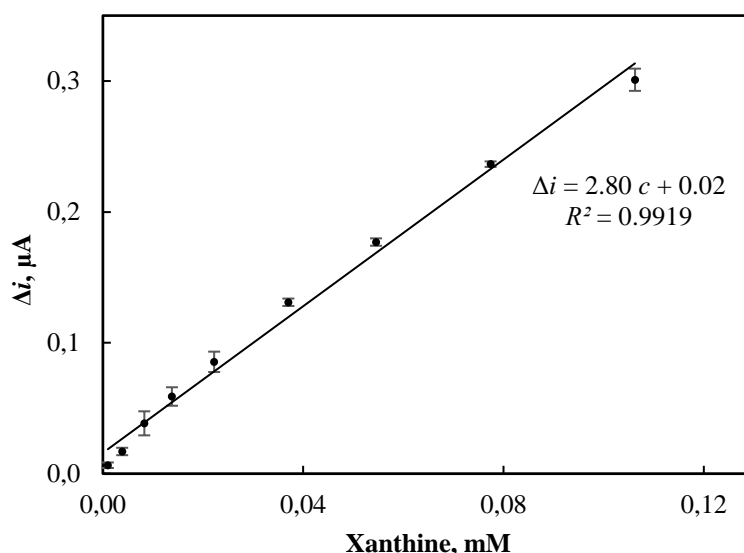


**Figure 6.** Calibration graph of XOx/BQ-MWCNTs-ZnO-CS/GCE after successive xanthine injections into a stirred solution of PBS (0.05 M; pH 7.5) at an operating potential of +0.25 V.

Successive calibration curves ( $n=5$ ) were obtained by the use of the same electrode to determine the repeatability of the xanthine biosensor. The relative standard deviation (RSD) of the sensitivity values was 4.0% revealing the good repeatability of the XOx/BQ-MWCNTs-ZnO-CS/GCE. The long-term stability of the XOx/BQ-MWCNTs-ZnO-CS/GCE was studied by recording the current response at a xanthine concentration of 0.5 mM over a period of 25 days. The biosensor was stored at 4 °C between the measurements under a dry atmosphere. The XOx/BQ-MWCNTs-ZnO-CS/GCE maintained 95% of the initial current response even after about 25 days. This suggests that use of BQ-MWCNTs-ZnO-CS composite ensures good stability of the biosensor.

The selectivity study of the XOx/BQ-MWCNTs-ZnO-CS/GCE was performed by comparing the amperometric response before and after the injection of various interferents such as glucose, ascorbic acid, sodium benzoate, uric acid, and creatine along with xanthine in 0.05 M PBS. Amperometric responses were obtained by injection of 0.03 mM xanthine and 0.01 mM interfering species. The interference was determined as the percentage of the current signal obtained for detecting 0.03 mM xanthine, which was contributed by the addition of a particular interfering substance. The results showed that, sodium benzoate, glucose, creatine, caffeine, and theophylline practically have no interference in the analysis of xanthine. The interference caused by ascorbic acid and uric acid to 0.03 mM xanthine was about 2% and 10% respectively. The good selectivity of the presented biosensor towards xanthine detection may be attributed to the low operating potential of +0.25 V and presence of Nafion layer that can minimize the interference effect.

To evaluate the performance of the presented xanthine biosensor, a comparison of different parameters obtained by various biosensors for xanthine detection are given in Table 1. The results

presented in this table show that the different characteristics of the proposed biosensor are better in some cases or comparable with the other xanthine biosensors reported so far.

### Analysis of meat samples

To evaluate the possible analytical application of the xanthine biosensor, the variation of xanthine content in meat samples with storage time was investigated.

For this purpose, chicken meat was chopped and homogenized. This homogenate was then portioned into five equal parts. One of these parts was then mechanically stirred for 45 min in 20 mL of deionized water for xanthine extraction and then centrifuged at 4000 rpm for 10 min. This homogenate was filtered through a Whatman filter membrane. The filtrate was diluted to 25.0 mL with deionized water. The same sample preparation route was applied to the other meat sample (beef). To study the effect of storage time on freshness of meat, the other parts were stored at +4°C up to 9 days and the samples were analyzed for xanthine concentration every 2 days. The xanthine concentration in chicken and beef meat were measured by the purposed biosensor at different storage times ranging from 1 to 9 days using the standard addition method. Aliquots of standard xanthine solution was added to several portions of the chicken and beef meat extracts, to obtain a multiple addition calibration curve. Xanthine concentration in chicken and beef meat extracts calculated from the calibration curves were  $0.36\pm 0.01$  and  $0.47\pm 0.01$  mg L<sup>-1</sup> ( $n=3$ ) on the first day, respectively. Figure 7 shows the results of the real sample analysis. It is clear from the figure that xanthine content increased with the storage time of meat samples. It was 5.4 times higher for the chicken sample and 1.6 times higher for the beef sample at day 9 than those at day 1. The increase in xanthine accumulation with storage time is an expected result (32). The experimental results indicated that the presented XOx/BQ-MWCNTs-ZnO-CS/GCE can be used for the monitoring of xanthine accumulation with storage time in meat samples.

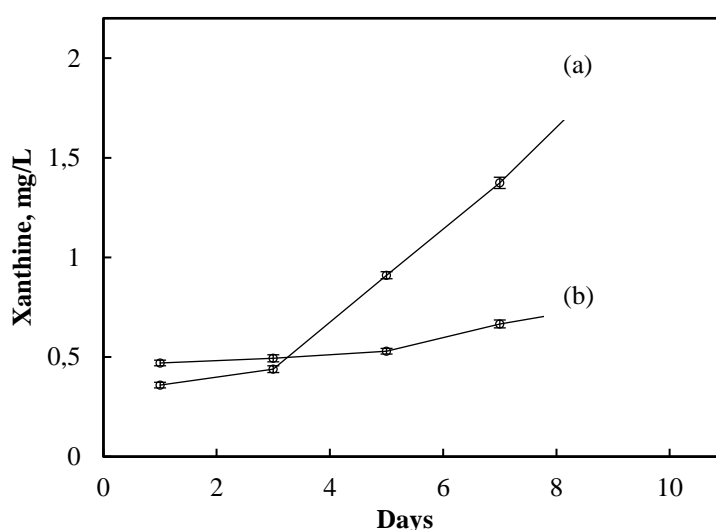


**Figure 7.** Variation of xanthine level in chicken (a) and beef (b) during storage at +4°C.

**Table 1.** Comparison of various amperometric xanthine biosensors reported in the last decade.

Enzyme /Working potential	Electrode composition/Immobilization technique	Linearity/Detection limit	Resp. time	Interf.	Storage stability	Ref.
XOx/−0.4V vs. SCE	Silica sol-gel film/XOx/CNT/GCE	0.2–10 μM/0.1 μM	6 s	–	5% loss after 90 days	[33]
XOx/0.05 V vs. Ag/AgCl	PB/SPTE/Cross-linking	$1 \times 10^{-7}$ – $4.98 \times 10^{-6}$ M /0.10 μM	–	–	–	[18]
XOx/−0.05 V vs. Ag/AgCl	Graphite electrode modified with platinum and and palladium	1.5–70 μM/ $1.5 \times 10^{-6}$ M	60 s	AA, UA (nr)	–	[27]
XOx/+0.4 V vs. Ag/AgCl	Au-NPs/PVF/Pt	$2.5 \times 10^{-6}$ – $5.6 \times 10^{-4}$ M/0.75 μM	–	AA (17.2%)	18 days (40% loss)	[26]
	Pt-NPs/PVF/Pt/Electro deposition	$2.0 \times 10^{-6}$ – $6.6 \times 10^{-4}$ M /0.60 μM		AA (20.5%)	23 days (40% loss)	
XOx/+0.5 V vs. Ag/AgCl	PVF-perchlorate matrix/Pt electrode/Electro deposition	$4.3 \times 10^{-7}$ – $2.84 \times 10^{-3}$ M/0.13 μM	15 s	AA, UA (nr)	25 days (42% loss)	[34]
XOx/+0.05 V vs. Ag/AgCl	Phenazine methosulfate as mediator/ Edge-plane pyrolytic graphite/ Adsorption	$1.0 \times 10^{-5}$ – $1.8 \times 10^{-3}$ M/0.25 nM	–	AA, UA (nr)	4 weeks (22% loss)	[35]
XOx/+0.25 V vs. Ag/AgCl	1,4-benzoquinone/CPE	$1.9 \times 10^{-7}$ – $5.5 \times 10^{-6}$ M and $5.2 \times 10^{-5}$ – $8.2 \times 10^{-4}$ M/0.1 μM	100 s	AA (18.2%), UA (3.6%)	14 days	[25]
		$1.9 \times 10^{-6}$ – $1.0 \times 10^{-5}$ M and $5.2 \times 10^{-5}$ – $8.2 \times 10^{-4}$ M/0.1 μM	50 s	AA(18.4%), UA (2.5%)	7 days	
XOx/+0.30 V vs. Ag/AgCl	PVF/CPE/Cross-linking					
XOx/+0.50 V vs. Ag/AgCl	CS/Fe-NPs@Au/PGE/Electro deposition	$1 \times 10^{-7}$ – $3 \times 10^{-4}$ M/0.1 μM	3s	AA (10%), UA (nr)	100 days (25% loss)	[1]
XOx/+0.50V vs. Ag/AgCl	Gold coated Fe-NPs/CS/Covalent immobilization	1–300 μM/0.1 μM	3s	AA (nr)	25% loss after 100 days	[36]
XOx/+0.35 V vs. Ag/AgCl	Poly(glycidyl methacrylate-co-vinylferrocene)/MWCNT/PGE/Covalent immobilization	$2 \times 10^{-6}$ – $2.8 \times 10^{-5}$ M; $2.8 \times 10^{-5}$ – $4.6 \times 10^{-5}$ ; $4.6 \times 10^{-5}$ – $8.6 \times 10^{-5}$ /0.12 μM	4 s	AA, UA (nr)	25 days (30% loss)	[28]
XOx/+0.25 V vs. Ag/AgCl	XOx/BQ-MWCNTs-ZnO-CS/GCE/Cross-linking	$9.0 \times 10^{-7}$ – $1.1 \times 10^{-4}$ M/ $2.1 \times 10^{-7}$ M	10 s	AA (2%), UA (10%)	25 days (5% loss)	This work

\*SPTE : screen-printed three-electrode; PVF : polyvinylidene fluoride; CPE: carbon paste electrode; PGE : pencil graphite electrode; nr:no response

## CONCLUSION

A new biosensor for xanthine analysis was developed based on the BQ-MWCNTs-ZnO-CS composite modified GCE. The proposed biosensor exhibited a low response time (10 s), satisfactory repeatability (4.0%), good sensitivity ( $39.4 \mu\text{A}/\text{mMcm}^2$ ), wide linear range ( $9.0 \times 10^{-7}$ – $1.1 \times 10^{-4}$  M), and low detection limit ( $2.1 \times 10^{-7}$  M). Moreover, the biosensor showed good selectivity due to the low operating potential. In conclusion, the presented biosensor can be utilized to detect the xanthine content in chicken and beef samples for the evaluation of meat freshness.

## ACKNOWLEDGMENTS

Financial support of this research Ankara University Research Fund (Project No: 16H0430007) is gratefully acknowledged.

## REFERENCES

1. Devi R, Batra B, Lata S, Yadav S, Pundir, CS. A method for determination of xanthine in meat by amperometric biosensor based on silver nanoparticles/cysteine modified Au electrode. *Process Biochem.* 2013; 48(2): 242–9.
2. Ronkainen NJ, Halsall HB, Heineman WR. Electrochemical biosensors. *Chem. Soc. Rev.* 2010; 39(5): 1747-63.
3. Anik Ü, Çubukçu M. Examination of the electroanalytic performance of carbon nanotube (CNT) modified carbon paste electrodes as xanthine biosensor transducers. *Turk. J. Chem.* 2008; 32: 711-9.
4. Jacobs CB, Peairs MJ, Venton, BJ. Review: Carbon nanotube based electrochemical sensors for biomolecules. *Anal. Chim. Acta* 2010; 662(2): 105-27.
5. Lin J, He C, Zhang L, Zhang S. Sensitive amperometric immunosensor for  $\alpha$ -fetoprotein based on carbon nanotube/gold nanoparticle doped chitosan film. *Anal. Biochem.* 2009; 384: 130–5.
6. Kaçar C, Dalkıran B, Erden PE, Kiliç E. An amperometric hydrogen peroxide biosensor based on Co<sub>3</sub>O<sub>4</sub> nanoparticles and multiwalled carbon nanotube modified glassy carbon electrode. *Appl. Surf. Sci.* 2014; 311: 139-46.
7. Palanisamy S, Cheemalapati S, Chen SM. Highly sensitive and selective hydrogen peroxide biosensor based on hemoglobin immobilized at multiwalled carbon nanotubes–zinc oxide composite electrode. *Anal. Biochem.* 2012; 429(2): 108-15.
8. Kavitha T, Gopalan AI, Lee KP, Park SY. Glucose sensing, photocatalytic and antibacterial properties of graphene–ZnO nanoparticle hybrids. *Carbon* 2012; 50(8): 2994-3000.
9. Wang YT, Yu L, Wang J, Lou L, Du WJ, Zhu ZQ, Peng H, Zhu JZ. A novel L-lactate sensor based on enzyme electrode modified with ZnO nanoparticles and multiwall carbon nanotubes. *J. Electroanal. Chem.* 2011; 661: 8-12.
10. Haghighi B, Bozorgzadeh S. Fabrication of a highly sensitive electrochemiluminescence lactate biosensor using ZnO nanoparticles decorated multiwalled carbon nanotubes. *Talanta* 2011; 85(4): 2189-93.

11. Ma W, Tian D. Direct electron transfer and electrocatalysis of hemoglobin in ZnO coated multiwalled carbon nanotubes and Nafion composite matrix. *Bioelectrochem.* 2010; 78(2): 106-12.
12. Zhang W, Yang T, Huang D, Jiao K, Li G. Synergistic effects of nano-ZnO/multi-walled carbon nanotubes/chitosan nanocomposite membrane for the sensitive detection of sequence-specific of PAT gene and PCR amplification of NOS gene. *J. Membr. Sci.* 2008; 325(1): 245-51.
13. Hu F, Chen S, Wang C, Yuan R, Chai Y, Xiang Y, Wang C. ZnO nanoparticle and multiwalled carbon nanotubes for glucose oxidase direct electron transfer and electrocatalytic activity investigation. *J. Mol. Catal. B: Enzym.* 2011; 72(3): 298-304.
14. Liu Y, Nie L, Tao W, Yao S. Full Paper Amperometric study of au-colloid function on xanthine biosensor based on xanthine oxidase immobilized in polypyrrole layer. *Electroanal.* 2004; 16: 1271-8.
15. Zhao J, O'daly JP, Henkens RW, Stonehuerner J, Crumbliss AL. A xanthine oxidase/colloidal gold enzyme electrode for amperometric biosensor applications. *Biosens. Bioelectron.* 1996; 11(5): 493-502.
16. Kilinc E, Erdem A, Gokgunec L, Dalbasti T, Karaoglan M, Ozsoz M. Buttermilk based cobalt phthalocyanine dispersed ferricyanide mediated amperometric biosensor for the determination of xanthine. *Electroanal.* 1998; 10(4): 273-5.
17. Arslan F, Yaşar A, Kılıç E. An amperometric biosensor for xanthine determination prepared from xanthine oxidase immobilized in polypyrrole film. *Artif. cells blood substit. biotechnol.* 2006; 34(1): 113-28.
18. Teng Y, Chen C, Zhou C, Zhao H, Lan M. Disposable amperometric biosensors based on xanthine oxidase immobilized in the Prussian blue modified screen-printed three-electrode system. *Sci. China Chem.* 2010; 53(12): 2581-6.
19. Dalkıran B, Kacar C, Erden PE, Kilic E. Amperometric xanthine biosensors based on chitosan-Co 3 O 4-multiwall carbon nanotube modified glassy carbon electrode. *Sens. Actuators B Chem.* 2014; 200: 83-91.
20. Zhang S, Wang N, Niu Y, Sun C. Immobilization of glucose oxidase on gold nanoparticles modified Au electrode for the construction of biosensor. *Sens. Actuators B Chem.* 2005; 109: 367-74
21. Jakobs RCM, Janssen LJJ, Barendrecht E. Hydroquinone oxidation and p-benzoquinone reduction at polypyrrole and poly-N-methylpyrrole electrodes. *Electrochim. Acta*, 1985; 30(10): 1313-21.
22. Pajkossy T, Jurczakowski R. Electrochemical impedance spectroscopy in interfacial studies. *Curr. Opin. in Electrochem.* 2010; 1: 53-8.
23. Mulchandani, A., Pan, A.S. and Wilfred, C. 1999. Fiber-Optic Enzyme Biosensor for Direct Determination of Organophosphate Nerve Agents. *Biotechnol. Prog.*, 15, 130-4.
24. Kanyong, P., Pemberton, R.M., Jackson, S.K. and Hart, J.P. 2013. Development of an amperometric screen-printed galactose biosensor for serum analysis. *Analytical Biochemistry* 435, 114-9.
25. Shan D, Wang Y, Xue H, Cosnier S. Sensitive and selective xanthine amperometric sensors based on calcium carbonate nanoparticles. *Sens. Actuators B Chem.* 2009; 136: 510-5.
26. Jain U, Narang J, Rani K, Chauhan N. Synthesis of cadmium oxide and carbon nanotube based nanocomposites and their use as a sensing interface for xanthine detection. *RSC Adv.* 2015; 5: 29675-83.
27. Erden P, Pekyardımcı Ş, Kılıç E. Amperometric enzyme electrodes for xanthine determination with different mediators. *Acta Chim. Slov.*, 2012; 59(4): 824-32.

28. Borisova B, Ramos, J, Díez, P, Sánchez, A, Parrado, C, Araque, E, Villalonga, R, Pingarrón, J.M. A Layer-by-Layer Biosensing Architecture Based on Polyamidoamine Dendrimer and Carboxymethylcellulose-Modified Graphene Oxide. *Electroanalysis* 2015; 27: 2131-8.
29. Baş SZ, Gulce H, Yıldız S, Gulce A. Amperometric biosensors based on deposition of gold and platinum nanoparticles on polyvinylferrocene modified electrode for xanthine detection. *Talanta* 2011; 87: 189-96.
30. Dodevska T, Horozova E, Dimcheva N. Design of an amperometric xanthine biosensor based on a graphite transducer patterned with noble metal microparticles. *Cent. Euro. J. Chem.* 2010; 8: 19-27.
31. Dervisevic M, Custiuc E, Çeviki E, Şenel M. Construction of novel xanthine biosensor by using polymeric mediator/MWCNT nanocomposite layer for fish freshness detection. *Food Chem.* 2015; 181: 277-83.
32. Devi R, Yadav S, Pundir CS. Au-colloids-polypyrrole nanocomposite film based xanthine biosensor. *Colloids Surf. A Physicochem. Eng. Asp.* 2012; 394: 38-45.
33. Gao Y, Shen C, Di J, Tu Y. Fabrication of amperometric xanthine biosensors based on direct chemistry of xanthine oxidase, *Mater. Sci. Eng. C* 2009; 29: 2213-6.
34. Bas S.Z, Gulce H, Yıldız S. Amperometric xanthine biosensors based on electrodeposition of platinum on polyvinylferrocenium coated Pt electrode, *J. Mol. Catal. B: Enzym* 2011; 72: 282-8.
35. Kalimuthu P, Leimkuhler S, Bernhardt P.V. Low-potential amperometric enzyme biosensor for xanthine and hypoxanthine, *Anal. Chem.* 2012; 84: 10359-65.
36. Devi R, Yadav S, Nehra R, Yadav S, Pundir C.S. Electrochemical biosensor based on gold coated iron nanoparticles/chitosan composite bound xanthine oxidase for detection of xanthine in fish meat, *J. Food Eng.* 2013; 115: 207-14.

